Behavioral Models of Frequency Pulling in Oscillators

M. Esmaeil Heidari and A. A. Abidi
Electrical Engineering Department
University of California, Los Angeles

***Abstract*— Based on the state equations of an RLC circuit and hard-limiting characteristics of a transconductor a method is introduced to study and simulate the pulling effect in differential LC oscillators. This method includes phase and amplitude disturbances all at once. The model is validated by measurement results and an example is given to illustrate the application of this method in verifying the real circuits.**

***Index Terms*— Oscillator, Adler's equation, pulling, injection, state equation out-phasing.**

I. INTRODUCTION

Any oscillator is vulnerable to pulling. In practical systems, periodic waveforms at different frequencies can find their way through parasitic paths into an oscillator circuit, and entrain it or modulate it. It need not be a voltage-controlled oscillator; even fixed frequency oscillators can be pulled or parasitically modulated. This is particularly evident on integrated circuit oscillators that are part of complex systems, where periodic waveforms that are generated on some part of the chip make their way, through parasitic paths, into the oscillator (Fig. 1). Van der Pol [1] knew that periodic stimuli can lock oscillators, but if the stimulus was weak, it would perturb, or pull, the oscillator from its free-running orbit without locking it. The more practically-inclined Adler ([2]) re-visited these differential equations for the special case of weak injection, and found expressions for the frequency range over which it locks the oscillator. Recent work [3] generalizes Adler's results to large injections. Other work [4][5][6] formulates pulling and locking in more precise mathematical terms, but while the results may help in the development of better simulators, they leave design engineers wanting for a simple, fast, and handy method to see how an oscillator responds to various possible injections. While SPICE-based simulations are too slow, a behavioral simulation may make sense provided it is reasonably accurate and does not mislead. In this paper, we describe our experience with behavioral models which, we will show, produce valuable results in real time.

We will start with an analysis similar to Razavi's [7] but assume that the nonlinear active circuit in the oscillator is a hard limiter. This models today's widely used on-chip differential *LC* oscillator very well. Later, we use this to simulate pulling in an oscillator that is part of a complex single-chip wireless transmitter. We also show that a more accurate but equally efficient behavioral model can be found from the state equations of the *LC* tank and a hard-limiting model of the differential pair. This becomes the workhorse in our simulations.

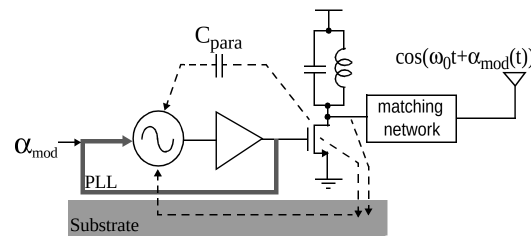

Fig. 1. Injection/pulling in a direct modulation transmitter

II. ADLER'S EQUATION IN THE DIFFERENTIAL *LC* OSCILLATOR

Fig. 2(a) shows the classic differential *LC* oscillator, with two current sources modeling injection into the output nodes. We assume a large enough steady-state amplitude that it forces the differential pair to commutate the tail current completely at its differential zero crossings. The differential current flowing into the LC tank is then $i = sgn(v_{out})I_0$, where sgn is the signum function. The two injection currents can always be decomposed into differential and common mode parts, and since the common mode is only important with a large nonlinear output capacitance when it converts AM into PM [3], it is neglected here. We assume that pulling arises mainly from the differential component.

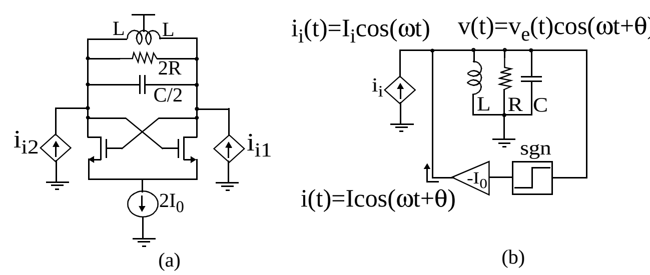

Fig. 2. (a) Differential LC oscillator with injected signal, (b) simplified model

Fig. 2(b) shows a simplified behavioral model of the LC oscillator. In this figure, $i_i = \dfrac{i_{i1} - i_{i2}}{2}$. The hard limiter passes phase modulation, but strips off amplitude modulation. It is triggered by zero crossings of the input, and produces a square wave current $\pm I_0$ that drives the LC tank circuit. The band-pass impedance produces a quasi-sinusoidal voltage. Thus, it is sufficient to consider only the fundamental component of current, $i(t) = \frac{4}{\pi} I_0 cos(\omega t + \theta) = Icos(\omega t + \theta)$, which produces an output voltage of the form $v(t) = v_e(t)cos(\omega t + \theta)$. This simplifies calculations without loss of generality.

By expressing periodic waveforms as complex variables, that is, $v(t) = v_e(t)e^{j\omega t}e^{i\theta}$, $i_i(t) = I_i e^{j\omega t}$ and $i(t) =$

$Ie^{j\omega t}e^{j\theta}$, we write KCL at the output node, and by equating real parts we get:

$$\frac{1}{R}\frac{dv_e}{dt} + \frac{1}{L}v_e + C\frac{d^2v_e}{dt^2} - C(\omega + \frac{d\theta}{dt})^2 v_e = I_i\omega sin(\theta) \quad (1)$$

Then noting that $v_e(t) \simeq RI = QL\omega I$ and $I_i \ll QI$, we simplify 1 into:

$$\frac{d\theta}{dt} = \omega_0 - \omega - \frac{\omega_0}{2Q}\frac{I_i}{I}\sin(\theta) \quad (2)$$

This is *Adler's equation*, with $\omega_0 = \sqrt{1/LC}$. From the analysis in [7] we can say that $\frac{I_i\omega_0}{2IQ} = \omega_L$ is the lock range. Injection within $\pm\omega_L$ of the free-running frequency will lock it to ω_{inj}.

III. System-level model of the LC oscillator with injection

In Fig. 2(b) KCL implies that:

$$\frac{1}{L}\int_{-\infty}^{t} v(t)dt + C\frac{dv(t)}{dt} + \frac{v(t)}{R} = i_t(t) \quad (3)$$

$i_t = i_i + i$ is the total current flowing into the tank. This can be re-arranged into

$$v(t) = R[i_t(t) - \frac{1}{L}\int_{-\infty}^{t} v(t)dt - C\frac{dv(t)}{dt}] \quad (4)$$

Fig. 3 is a signal flowgraph of state equation (4). A square wave multiplies the tail current to model commutation. The commutated current adds to the injected signal to generate i_t. Injection into the tail node (Fig. 2) at very low frequencies or near the second harmonic pulls the oscillator, because commutation by the differential pair shifts its frequency when it reaches the LC tank.

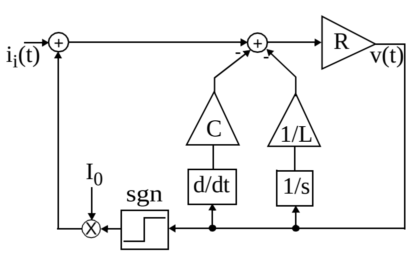

Fig. 3. Behavioral model of an LC oscillator with injected signal

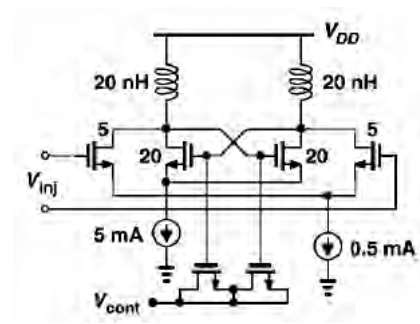

Fig. 4. Schematic of LC VCO ([7])

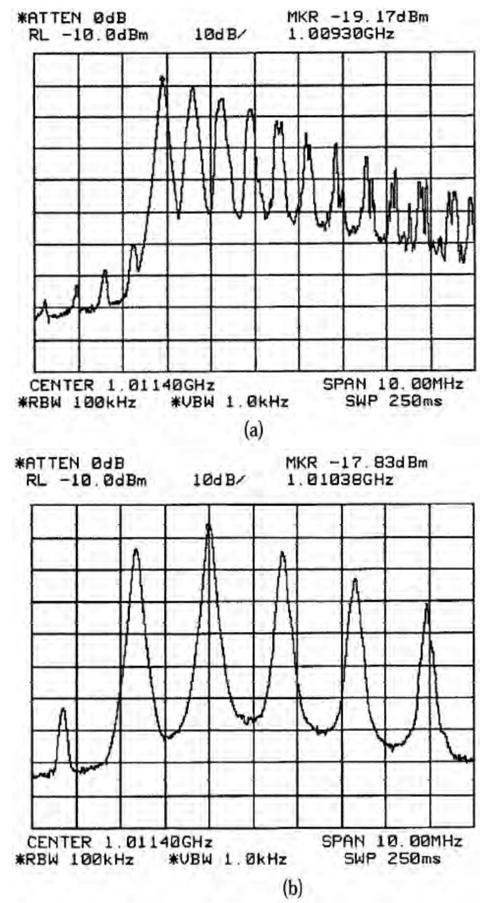

Fig. 5. Measured spectrum of free-running oscillator under injection ([7]). (a) Quasi-lock. (b) Fast beat.

IV. Predictions versus Measurements: Single oscillator

We validate the behavioral model (Fig. 3) of a standalone differential LC oscillator circuit under injection (Fig. 4) against the measurements reported in [7]. The parameters in the MATLAB simulation must reproduce the measurement conditions. For a sample of simulation set up including the schematic in SIMULINK environment and MATLAB code see Fig. 7 and Fig. 8. From the measured lock range of ± 1.5 MHz, we determine that the injection amplitude is almost 38 dB lower than the oscillation amplitude. In the first and second experiments, the injection frequency is chosen to be 110 kHz and 710 kHz *outside* the lock range (Fig. 5(a) and (b)). In the code shown in Fig. 8, lock range is set to the experimental value of ± 1.5 MHz which is slightly different from what equation 2 predicts.

Fig. 6 shows the simulation results. It is striking how well behavioral simulation reproduces the features of the pulled oscillator's measured spectrum (Figs. 5 and 6).

V. Behavioral Model of a complete system: Outphasing wireless transmitter

The power of behavioral modeling is manifest in simulating a complete system, which contains one or more oscillators among other building blocks. We model a LINC, or outphasing, transmitter, that reconstructs arbitrary amplitude and phase

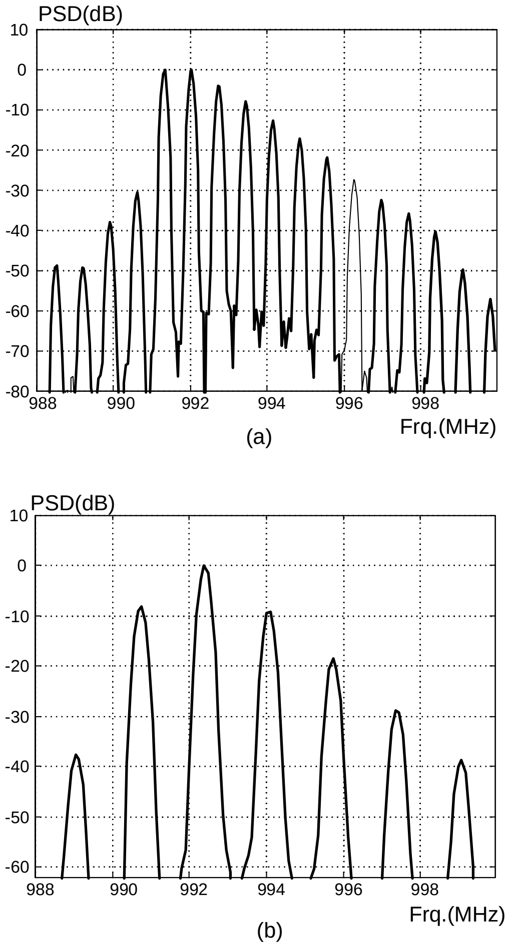

Fig. 6. Simulated spectrum of free running oscillator under injection. (a) Quasi-lock. (b) Fast beat.

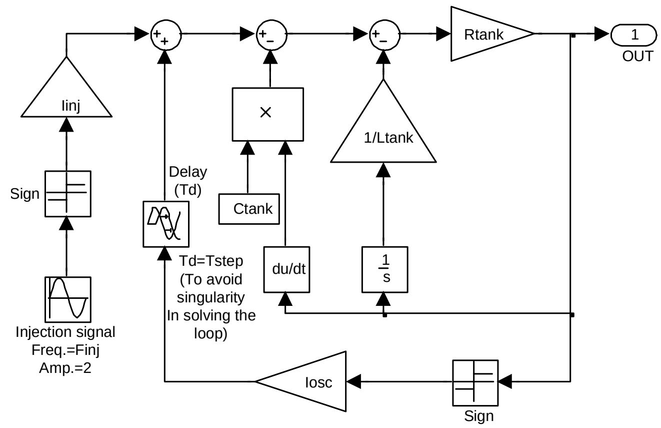

Fig. 7. *LC* oscillator model and injected signal in SIMULINK

```
Iosc=2.5e-3;        % tail current
F0=1e9;             % nominal oscillation frequency
Fosc=992936860; % actual oscillation frequency
                    % measured under "no-pulling" condition
Flock=1.5e6;        % lock range
Iinj=Iosc/80;       % Iinj(dB) = Iosc(dB)- 38

Qtank= 5.8;         % Quality factor of inductor
Ltank = 20e-9;      % inductor
Rtank=Qtank*Ltank*(2*pi*F0);  % parallel resistor  of tank
Ctank=1/(Ltank*(2*pi*F0)^2);    % capacitor

Tstep=(1/F0)/200;     % time step of simulation
Tmax=(2^21)*Tstep;  % simulation time
Finj=Fosc-Flock-710e3; % frequency of injected signal

sim('simulink_model_of_osc',Tmax)
Tx=out(ns:length(out));
Length_sim=length(Tx);
win=kaiser(Length_sim,20);  % Kaiser window
wTx=Tx.*win;
mTx=abs(fft(wTx')).^2;
mTx=mTx/max(mTx);

% Plotting the output spectrum
Fs=1/Tstep;
df=Fs/Length_sim;
f=df:df:Fs;
f1=F0-12e6;
f2=F0-0e6;
n1=floor(f1/df);
n2=floor(f2/df);
plot(f(n1:n2)-df,10*log10(mTx(n1:n2)),'k')
```

Fig. 8. MATLAB code for simulating model of Fig. 7

modulations by adding together the outputs of two power amplifiers, each driven by purely phase modulated waveforms at the carrier frequency. Since each amplifier outputs power at a constant envelope, it can be biased in compression for peak efficiency. This is an intriguing scheme to build an externally linear power amplifier with efficient but nonlinear components ([8], [9], [10]), but so far it has not entered the mainstream because of a variety of unresolved problems, such as how to combine power from the two amplifiers without loss. We believe that with recent advances in RF and mixed-signal integration, its time has come.

An obvious way to generate the phase-modulated carriers that drive the PAs is with two oscillators embedded in independent phase-locked loops (PLLs), each modulated within its loop. When the modulation bandwidth exceeds the loop bandwidth, as it inevitably will for systems beyond GSM, the input signal must be pre-emphasized to compensate for the 20 dB/decade roll off beyond the narrow loop bandwidth ([11]).

In a system as complex as this one, the oscillators can be pulled in a number of ways. For example, the high power output of a PA driven by one oscillator might couple, through on-chip parasitic paths like those shown in Fig. 1, into the other oscillator. Or the combined power output, which is amplitude and phase modulated, may couple into both oscillators. Before building this system, we were interested to simulate the impact of pulling on the transmitted output spectrum under various likely parasitic couplings. This is only practical using behavioral models. Thus the model of the oscillator was extended, first to embed it in a modulation PLL, and then into the full transmitter.

To model the varactor, a fraction of the LC tank capacitance is given a voltage dependence (Fig. 10). If needed, the characteristic of the VCO's frequency vs. voltage can be made nonlinear.

To complete the PLL model we add behavioral models

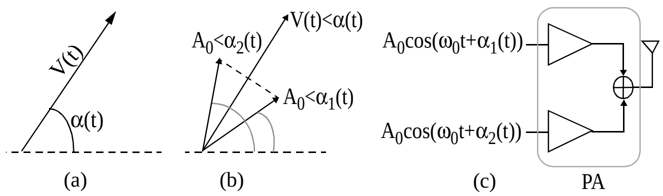

Fig. 9. LINC modulation, (a) variable envelope signal (b) decomposing the signal to two constant envelope signals (c)Power combining

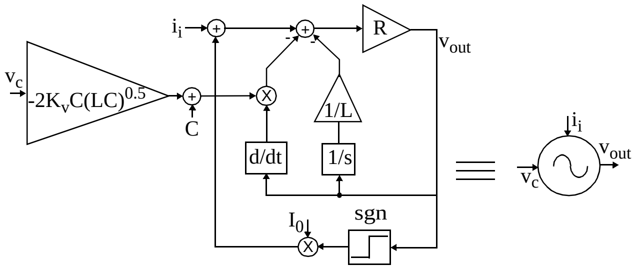

Fig. 10. VCO model with injection.

of the equalizer, loop filters and an ideal phase detector. The model of the phase detector (Fig. 11) is largely self-explanatory. In the actual realization, a time-to-digital converter, that is, a time-interval digitizer, measures phase. The behavioral model converts the time interval between successive falling edges of the reference and the VCO outputs into levels that represent samples of the evolving phase, and then it takes the difference in these levels. This is the true phase difference. The complete transmitter model is shown in Fig. 12. The sum of the two PLL outputs represents two ideal, non-interacting PAs whose output powers add without loss. In a LINC transmitter, the total power in two constant envelope waveforms reconstructs the desired amplitude- and phase-modulated power waveform.

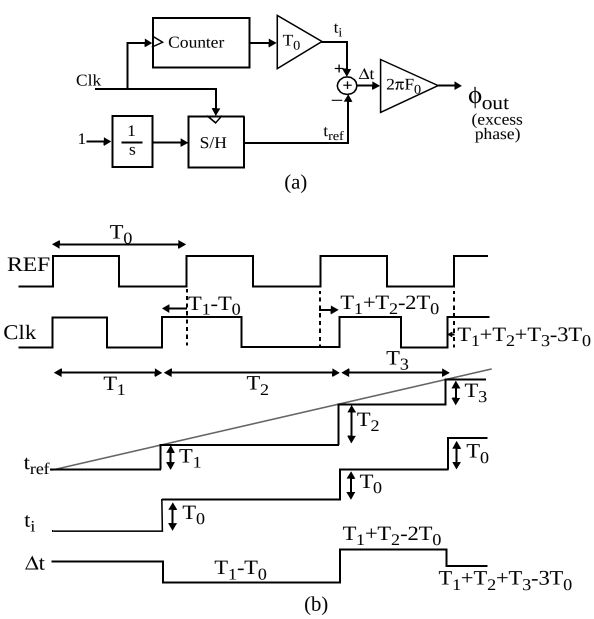

Fig. 11. Behavior model for phase detector

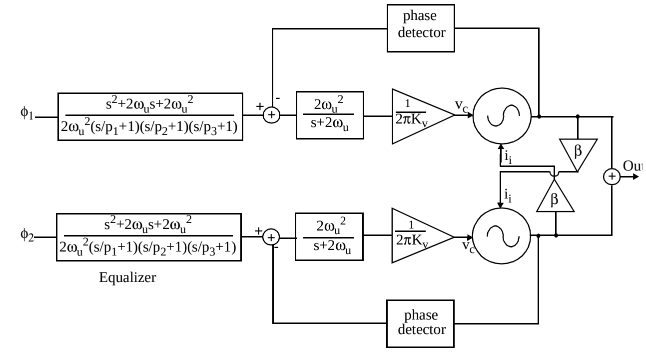

Fig. 12. Outphasing transmitter, behavioral model

Two independently modulated VCOs can pull each other through parasitic on-chip coupling. This pulling will likely be the main effect that limits spectral purity of the transmitter output. Behavioral models of pulling show this clearly (Fig. 14). The transmitter output spectra are compared to an ideal EDGE-modulated spectrum. To model parasitic injection, the output of one VCO is attenuated and added to the other VCO's output. An injection level 80 dB smaller than the VCO amplitude produces the spectrum shown in the same figure. Clearly even this very weak coupling erodes all the margin between the output spectrum and the transmit mask.

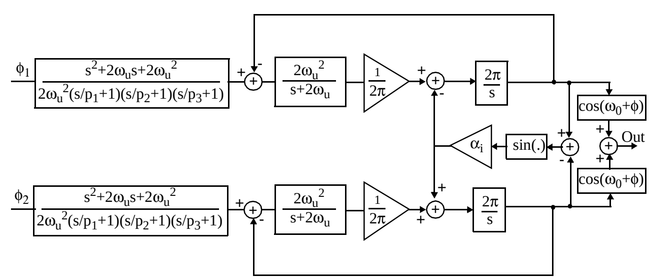

Fig. 13. Outphasing transmitter, linear model (equation 2)

Whereas simulation of the entire transmitter in SPICE is intractable, in MATLAB or VERILOG-A it is quite manageable; indeed it is fast. In the early stages of investigation while the design space is being explored, even this model may be unnecessarily detailed. In this case we will show that a simpler linear model is, in many cases, sufficient.

As Fig. 13 shows, we can use Adler's equation 1 to model an oscillator pulled by weak injection. Fig. 14 compares simulations with this simple linear model and the more realistic model of Fig. 12. The two are off by a few dB because Adler's equation does not account for amplitude disturbances. In an outphasing transmitter, amplitude fluctuations translate into unwanted phase variations, resulting in spectral regrowth.

The linear model gives a good enough idea of whether or not the transmitter will work. The design can be refined with more comprehensive behavioral simulations, which form the basis of an IC realization.

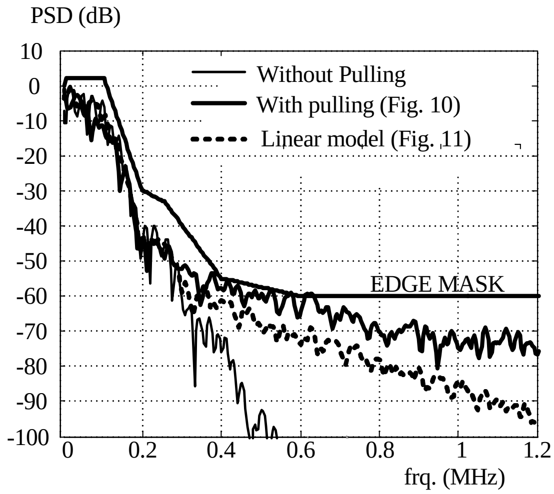

Fig. 14. Simulation results (a) with and without pulling (b) Linear vs. precise model $I_{inj}/I_{osc} = -80dB$

VI. Conclusion

After a brief study of the mechanisms of pulling in a highly nonlinear LC oscillator, we present simple behavioral models that capture this well in a differential LC oscillator. The models are put to use to predict how parasitic pulling may corrupt the output of an outphasing, or LINC, wireless transmitter. An IC prototype transmitter has been realized based on this model.

The authors thank Shervin Moloudi for comments.

References

[1] B. Van der Pol, "Forced oscillations in a circuit with nonlinear resistance," *Phil. Mag.*, vol. 3, pp. 65–80, 1920.

[2] R. Adler, "A study of locking phenomena in oscillators," *Proceedings of the IRE*, vol. 34, no. 6, pp. 351–357, June 1946.

[3] A. Mirzaei, M. E. Heidari, and A. A. Abidi, "Analysis of oscillators locked by large injection signals: Generalized adlers equation and geometrical interpretation," in *Conference 2006, IEEE Custom Integrated Circuits*, San Jose, CA, Sept. 2006, pp. 737–740.

[4] X. Lai and J. Roychowdhury, "Automated oscillator macromodelling techniques for capturing amplitude variations and injection locking," *2004. ICCAD-2004. IEEE/ACM International Conference on Computer Aided Design*, pp. 687–694, Nov. 2004.

[5] ——, "Analytical equations for predicting injection locking in LC and ring oscillators," in *Custom Integrated Circuits Conference, 2005. Proceedings of the IEEE 2005*, Sept. 2005, pp. 461–464.

[6] T. Mei and J. Roychowdhury, "Rigorous analytical/graphical injection locking analysis of two-port negative resistance oscillators," in *Conference 2006, IEEE Custom Integrated Circuits*, San Jose, CA, Sept. 2006, pp. 741–744.

[7] B. Razavi, "A study of injection locking and pulling in oscillators," *IEEE Journal of Solid-State Circuits*, vol. 39, no. 9, pp. 1415–1424, Sept. 2004.

[8] H. Chireix, "High power outphasing modulation," *Proceedings of the IRE*, vol. 23, no. 11, pp. 1370–1392, Nov. 1935.

[9] D. Cox, "Linear amplification with nonlinear components," *Communications, IEEE Transactions on [legacy, pre - 1988]*, vol. 22, no. 12, pp. 1942–1945, Dec. 1974.

[10] A. Bateman, "The combined analogue locked loop universal modulator (CALLUM)," in *Vehicular Technology Conference, 1992 IEEE 42nd*, Denver, CO, May 1992, pp. 759–763.

[11] M. H. Perrott, I. Tewksbury, T. L., and C. G. Sodini, "A 27-mw CMOS fractional-n synthesizer using digital compensation for 2.5-mb/s GFSK modulation," *IEEE Journal of Solid-State Circuits*, vol. 32, no. 12, pp. 2048–2060, Dec. 1997.